Hindawi
Bioinorganic Chemistry and Applications
Volume 2022, Article ID 1817745, 10 pages
https://doi.org/10.1155/2022/1817745

Research Article

Molecular Insights into How the Dimetal Center in Dihydropyrimidinase Can Bind the Thymine Antagonist 5-Aminouracil: A Different Binding Mode from the Anticancer Drug 5-Fluorouracil

En-Shyh Lin,[1] **Ren-Hong Luo**,[2] **Ya-Ching Yang**,[2] **and Cheng-Yang Huang**[2,3]

[1]*Department of Beauty Science, National Taichung University of Science and Technology, Taichung City, Taiwan*
[2]*School of Biomedical Sciences, Chung Shan Medical University, Taichung City, Taiwan*
[3]*Department of Medical Research, Chung Shan Medical University Hospital, Taichung City, Taiwan*

Correspondence should be addressed to Cheng-Yang Huang; cyhuang@csmu.edu.tw

Received 3 November 2021; Accepted 27 January 2022; Published 14 February 2022

Academic Editor: Jamal Rafique

Dihydropyrimidinase (DHPase) is a key enzyme for pyrimidine degradation. DHPase contains a binuclear metal center in which two Zn ions are bridged by a posttranslationally carbamylated lysine. DHPase catalyzes the hydrolysis of dihydrouracil to *N*-carbamoyl-*β*-alanine. Whether 5-aminouracil (5-AU), a thymine antagonist and an anticancer drug that can block DNA synthesis and induce replication stress, can interact with DHPase remains to be investigated. In this study, we determined the crystal structure of *Pseudomonas aeruginosa* DHPase (PaDHPase) complexed with 5-AU at 2.1 Å resolution (PDB entry 7E3U). This complexed structure revealed that 5-AU interacts with Zn*α* (3.2 Å), Zn*β* (3.0 Å), the main chains of residues Ser289 (2.8 Å) and Asn337 (3.3 Å), and the side chain of residue Tyr155 (2.8 Å). These residues are also known as the substrate-binding sites of DHPase. Dynamic loop I (amino acid residues Pro65-Val70) in PaDHPase is not involved in the binding of 5-AU. The fluorescence quenching analysis and site-directed mutagenesis were used to confirm the binding mode revealed by the complexed crystal structure. The 5-AU binding mode of PaDHPase is, however, different from that of 5-fluorouracil, the best-known fluoropyrimidine used for anticancer therapy. These results provide molecular insights that may facilitate the development of new inhibitors targeting DHPase and constitute the 5-AU interactome.

1. Introduction

Pyrimidine bases are essential for the replication of genetic information, cellular metabolism, and cell growth in all biological systems [1]. Uracil derivatives, especially 5-substituted uracils, play a significant role in pharmacological activities, such as antiviral [2], anticancer drugs [3], antibacterial [4], anti-inflammatory [5, 6], and antitumor activities [7–9]. For example, 5-fluorouracil (5-FU) is an FDA-approved drug with a remarkable therapeutic effect for the systemic treatment of cancers of the gastrointestinal tract, breast, head, and neck in the clinic [8]. As a thymine antagonist possessing anticancer activities, 5-aminouracil (5-AU) can block DNA synthesis and induce replication stress [10, 11]. In addition, recent findings indicate that microbiota can modulate the host response to these chemotherapeutic drugs [12]. Thus, the whole interactome of these five-substituted uracil drugs should be determined for detailed clinical pharmacokinetic and toxicity analyses.

Dihydropyrimidinase (DHPase) [13] is a key enzyme for pyrimidine degradation (Figure 1(a)). DHPase contains a binuclear metal center in which two Zn ions are bridged by a posttranslationally carbamylated lysine (Kcx) [14–18]. DHPase catalyzes the hydrolysis of dihydrouracil (DHU) to *N*-carbamoyl-*β*-alanine. Including a Kcx, the dimetal center (Zn*α*/Zn*β*) of DHPase consists of four His and one Asp. The conserved substrate binding sites of DHPase are Ser, Asn, and Tyr [19]. Of these residues, Ser and Asn interact with the

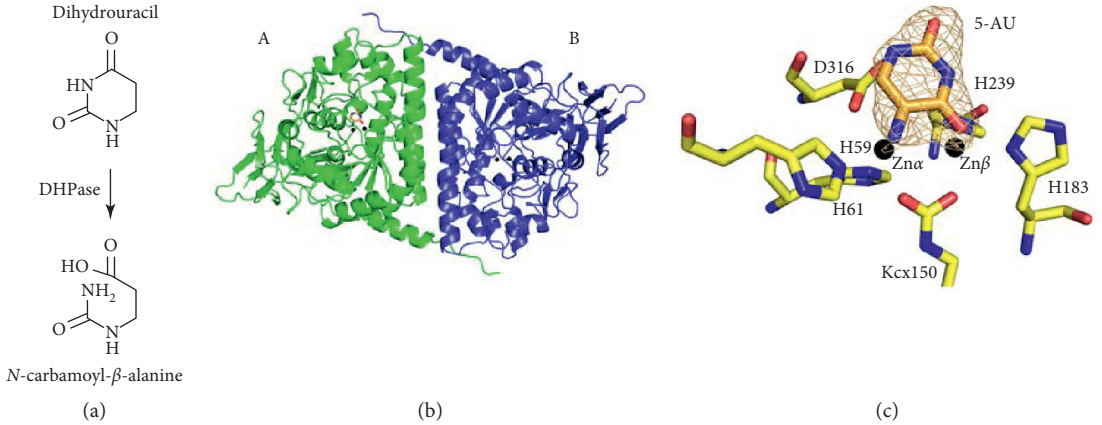

Figure 1: The structure of PaDHPase complexed with 5-AU. (a) The physiological reaction of DHPase. (b) The complexed structure of PaDHPase with 5-AU. The monomers are colored differently. 5-AU was found only in monomer A and not in monomer B. (c) The active site of PaDHPase. The binuclear metal center assembled by residues His59, His61, carbamylated Lys150 (Kcx150), His183, His239, and Asp316 in PaDHPase is essential for catalytic activity. The light orange mesh is the 2Fo-Fc electron density map from the 5-AU contoured at 1σ with a 1.6 Å carve radius. Both two zinc ions were involved in binding 5-AU.

substrate DHU through the backbone of DHPase. Despite the interactions via the main chain, mutations of these residues still lead to severely impaired enzymes [16]. Loss of the Znβ ion causes Kcx to no longer be carbamylated in mono-Zn DHPase [14]. On the basis of an analysis of the amino acid sequences, DHPase was suggested to be a member of the cyclic amidohydrolase family [20, 21]. The cyclic amidohydrolase family also includes dihydroorotase [22–28], allantoinase [28–30], hydantoinase [31, 32], and imidase [33–35]. These metal-dependent enzymes catalyze the hydrolysis of the cyclic amide bond of each substrate in the metabolism of purines and pyrimidines. Some of these amidohydrolases are known to be anticancer [24, 36–38], antimicrobial [16, 27, 39], and antimalarial targets [40, 41] because of their involvement in the key reactions of nucleotide synthesis. Therefore, new inhibitors should be found, and their binding modes should be investigated for chemotherapeutic drug development.

5-FU-associated toxicity was reported [42]. After treatment of 5-FU for anticancer therapy, the asymptomatic patients with DHPase deficiency suffered from severe toxicity, including death [43]. A recent report revealed that DHPase is a novel 5-FU-binding protein [44]. Whether and how other five-substituted uracil drugs such as 5-AU can bind to DHPase remains to be elucidated. In the present study, we found that 5-AU can bind to *Pseudomonas aeruginosa* DHPase (PaDHPase). We determined the crystal structure of the PaDHPase complex with 5-AU at a 2.1 Å resolution (PDB entry 7E3U). Given the structural resemblance between 5-FU and 5-AU, one might conclude that the mode of 5-FU bound by PaDHP must be similar to that of 5-AU. However, we found that their binding modes are different. The fluorescence quenching method and site-directed mutagenesis were also used to confirm the binding mode of 5-AU to PaDHPase revealed by the complex structure. We think that the determination of this complex structure can extend the knowledge of the 5-AU interactome and benefit anticancer development.

2. Materials and Methods

2.1. Expression and Purification of PaDHPase. The expression vector pET21b-PaDHPase [16] was transformed into *Escherichia coli* BL21 (DE3) cells and grown in LB medium at 37°C. The overexpression was induced by incubating with 1 mM isopropyl thiogalactopyranoside for 9 h. Recombinant PaDHPase [36] was purified from the soluble supernatant by using Ni^{2+}-affinity chromatography (HiTrap HP; GE Healthcare Bio-Sciences). The recombinant protein was eluted with a linear imidazole gradient and dialyzed against a dialysis buffer (20 mM Tris-HCl and 0.1 M NaCl, pH 7.9; Buffer A).

2.2. Preparation of Mono-Zn PaDHPase (Znα-PaDHPase). The mono-Zn PaDHPase was prepared using the protocol described previously [45]. Purified PaDHPase was dialyzed against a chelating buffer (50 mM MES, 50 mM EDTA, and 15 mM 8-HQSA, pH 6.5; Buffer B) at room temperature for 3 days. The resultant enzyme solution was then dialyzed against Buffer A.

2.3. Site-Directed Mutagenesis. The PaDHPase mutants were generated according to the QuikChange Site-Directed Mutagenesis kit protocol (Stratagene; La Jolla, CA, USA). The wild-type plasmid pET21b-PaDHPase was used as a template [16]. The presence of the mutation was verified by DNA sequencing in each construct. The recombinant mutant proteins were purified using the protocol for the wild-type PaDHPase by Ni^{2+}-affinity chromatography (Table 1).

2.4. Crystallography. The optimal protein concentration for crystallization of the PaDHPase complex, determined by the Pre-Crystallization Test (Hampton), was 10 mg/mL. Crystals were grown at room temperature by hanging drop vapor diffusion in 16% PEG 8000, 100 mM HEPES, 200 mM

Table 1: Primers used for construction of plasmids.

Oligonucleotide	Primer
Y155A-N	CACTTCATGGCCGCCAAGAACGCCATCATGGCC
Y155A-C	CATGATGGCGTTCTTGGCGGCCATGAAGTGCTT
S289A-N	GGCTACGTGATGGCCCCGCCGTTCCGTCCCGTC
S289A-C	GGGACGGAACGGCGGGGCCATCACGTAGCCGGC
C318A-N	CCGCCACCGACCACGCCTGCTTCTGCGCCGAGC
C318A-C	CGCAGAAGCAGGCGTGGTCGGTGGCGGTGGTAT
N337A-N	TTCAGCAAGATTCCCGCTGGCACGGCCGGCATC
N337A-C	GCCGGCCGTGCCAGCGGGAATCTTGCTGAAGTC

These plasmids were verified by DNA sequencing. Underlined nucleotides indicate the designated site for mutation or the restriction site.

calcium acetate, and 200 μM 5-AU, at pH 7.5. Data were collected using an ADSC Quantum-315r CCD area detector at SPXF beamline BL13C1 at the National Synchrotron Radiation Research Center (NSRRC; Hsinchu, Taiwan). The structure of the 5-AU-PaDHPase complex was solved to 2.1 Å resolution with the molecular replacement software Phaser-MR [46] using PaDHPase (PDB entry 5E5C) [15] as a model (Table 2). The data were indexed and scaled using HKL-2000 [47]. Models were built and refined with PHENIX [48] and Coot [49]. Coordinate and structure factor files have been deposited in the Protein Data Bank (PDB entry 7E3U).

2.5. Determination of the Dissociation Constant (K_d). Through the fluorescence quenching analysis, the K_d value of the purified PaDHPase was determined [44]. An aliquot of 5-AU was added into the solution containing PaDHPase (0.8 μM) and 50 mM HEPES at pH 7.0. The decrease in the intrinsic fluorescence of PaDHPase was measured at 336 nm upon excitation at 279 nm and 25°C with a spectrofluorimeter (Hitachi F-2700; Hitachi High-Technologies, Japan). The K_d was obtained using the equation: $\Delta F = \Delta F_{max} - K_d(\Delta F/[5\text{-AU}])$.

3. Results and Discussion

3.1. Crystallization of the PaDHPase-5-AU Complex. PaDHPase crystals can be obtained by hanging drop vapor diffusion in 28% PEG 6000, 100 mM HEPES, and 200 mM lithium acetate at pH 7.5 [15]. Soaking and cocrystallization of PaDHPase with 5-AU under these conditions were attempted but were unsuccessful. After crystallization screening, the crystals of the PaDHPase-5-AU complex appeared at room temperature in 16% PEG 8000, 100 mM HEPES, 200 mM calcium acetate, and 200 μM 5-AU, at pH 7.5. These crystals were used for determining the complex structure of PaDHPase.

3.2. Structure of PaDHPase in Complex with 5-AU. The crystals of the 5-AU-PaDHPase complex belong to space group $P3_12_1$ with cell dimensions of $a = 112.67$, $b = 112.67$, and $c = 161.43$ Å. The complexed crystal structure of PaDHPase with 5-AU was determined at a 2.1 Å resolution (Table 2). Two monomers of PaDHPase were found in the asymmetric unit (Figure 1(b)). Consistently, PaDHPase functions as a dimer [15]. The electron density of 5-AU was well defined and indicated the presence of 5-AU in the active site of PaDHPase (Figure 1(c)). The orientation of 5-AU could be easily distinguished on the basis of the location of the substituent. However, only one 5-AU molecule was found in the active site of one of the PaDHPase dimers. This is also the case for 5-FU bound to PaDHPase [44]. The binding of 5-AU does not influence the overall structure of PaDHPase. Similar to the apo form, the global architecture of the 5-AU-complexed PaDHPase monomer (subunit A) revealed a TIM-barrel structure embedding the catalytic dimetal center (Znα and Znβ) and a β-sandwich domain, consisting of 17 α-helices, 19 β-sheets, 2 Zn ions, and 1 5-AU molecule. Both of the two zinc ions are involved in binding 5-AU. The dimetal center in the PaDHPase-5-AU complex

Table 2: Data collection and refinement statistics.

Data collection	
Crystal	PaDHP-5AU
Wavelength (Å)	1.0
Resolution (Å)	30–2.16
Space group	$P3_12_1$
Cell dimension a, b, c (Å)/β (°)	112.67, 112.67, 161.43/90
Redundancy	4.9 (4.9)
Completeness (%)	99.9 (99.9)
$<I/\sigma I>$	23.7 (3.1)
$CC_{1/2}$	0.965(0.866)
Refinement	
Resolution (Å)	29.01–2.16
No. of reflections	64183
R_{work}/R_{free}	0.185/0.229
No. of atoms	
Ligands	1
Protein	954
Zinc	4
Water	459
r.m.s deviations	
Bond lengths (Å)	0.008
Bond angles (°)	0.893
Ramachandran plot	
Favored (%)	95.45
Allowed (%)	3.7
Outliers (%)	0.85
PDB entry	7E3U

Values in parentheses are for the highest resolution shell. $CC_{1/2}$ is the percentage of correlation between the intensities of random half-data sets.

consisted of His59, His61, Kcx150, His183, His239, and Asp316 still self-assembles (Figure 1(c)). Lys150 remains carbamylated (Kcx150) regardless of 5-AU binding.

3.3. 5-AU Binding Mode. As a uracil derivative possessing many chemotherapeutic and pharmacological activities [11], 5-AU was identified as a ligand bound by PaDHPase in this study. The 5-AU binding mode of PaDHPase was demonstrated by the complexed crystal structure. On the basis of our crystallographic analysis, various interactions between 5-AU and PaDHPase were examined (Figure 2(a)). Residues Tyr155, Ser289, and Asn337 of PaDHPase, crucial for substrate binding [17, 19], are also involved in 5-AU binding (Figure 2(b)). 5-AU interacts with Znα (3.2 Å), Znβ (3.0 Å), the main chains of residues Ser289 (2.8 Å) and Asn337 (3.3 Å), and the side chain of residue Tyr155 (2.8 Å). Dynamic loop I (amino acid residues Pro65-Val70) in PaDHPase is not involved in the binding of 5-AU.

3.4. Structural Comparison of the Active Sites between the 5-AU Bound State and the 5-FU Bound State of PaDHPase. Recently, the crystal structure of PaDHPase in complex with the anticancer drug 5-FU was reported [44]. 5-FU is the best-known fluoropyrimidine used to target the enzyme thymidylate synthase in anticancer therapy [3, 8]. Given the structural similarity between 5-AU and 5-FU (Figure 3(a)), one might conclude that their binding mode by PaDHPase must be similar. The dynamic loops of PaDHPase extend toward the active site when either 5-FU or 5-AU is bound (Figure 3(b)). However, we found that 5-AU and 5-FU binding poses to PaDHPase are different in terms of orientation (Figure 3(b)) and binding residues (Figure 3(c)). The side chain of residue Cys318 in PaDHPase (Figure 3(d)) is involved in binding 5-FU (2.9 Å) but not 5-AU (Figure 2). In addition, the binding contributions from the metal ions in PaDHPase are different. Znβ is not involved in binding 5-FU [44], whereas both Zn ions interact with 5-AU (Figure 2). Thus, we concluded that the binding mechanisms of the anticancer drugs 5-FU and 5-AU to PaDHPase are different.

3.5. 5-AU Binding Analysis. Prior to this study, whether 5-AU could bind to DHPase remained unknown. To confirm if PaDHPase is capable of binding 5-AU, we used the fluorescence quenching method to determine the binding ability of PaDHPase (Figure 4). Quenching is a complex formation process that decreases the fluorescence intensity of protein. The fluorescence emission spectra of the wild-type PaDHPase was significantly quenched with 5-AU (Figure 4(a)). PaDHPase displayed strong intrinsic fluorescence with a peak wavelength of 336 nm when excited at 279 nm. When 5-AU was titrated into the PaDHPase solution, the intrinsic fluorescence of the protein was progressively quenched. Upon the addition of 300 μM 5-AU, the intrinsic fluorescence of PaDHPase was quenched by 87.3%. Adding 5-AU resulted in a red shift in the PaDHPase emission wavelength (~6.5 nm; λ_{max} from 336.5 to 343 nm). These observations indicated that PaDHPase can form a stable complex with 5-AU. As determined through the titration curve, the dissociation constant (K_d) of PaDHPase bound to 5-AU is 97.7 ± 2.0 μM. Based on the K_d value of PaDHPase bound to 5-FU (133.2 ± 8.5 μM) [44], PaDHPase may prefer binding to 5-AU over 5-FU.

3.6. Structure-Based Mutational Analysis. The complexed structure revealed Tyr155, Ser289, and Asn337 of PaDHPase as the 5-AU binding sites (Figure 2). 5-AU interacts with the main chains of residues Ser289 and Asn337 and the side chain of residue Tyr155. To investigate the contribution of individual amino acid residues to 5-AU binding, alanine substitution mutants (Table 2) were constructed and analyzed by fluorescence quenching (Figures 4(b)–4(d)). We found that 300 μM 5-AU quenched the intrinsic fluorescence of mutants Y155A, S289A, and N337A by 68.6%, 61.6%, and 72.4%, respectively. The K_d values of Y155A, S289A, and N337A bound to 5-AU were reduced to 247.1 ± 4.0, 256.0 ± 3.2, and 192.1 ± 8.0 μM, respectively. Accordingly, Ser289 is the most effective one of these residues for 5-AU binding.

Structurally, Cys318 is involved in 5-FU [44] but not 5-AU. For comparison, the C318A mutant was also analyzed by fluorescence quenching (Figure 4(e)). We found that 300 μM 5-AU quenched the intrinsic fluorescence of C318A by 86.8%. The K_d value of C318A was determined as 103.3 ± 3.1 μM. The abilities of the wild-type PaDHPase and the C318A mutant to bind 5-AU are approximately equal. Thus, Cys318 is not essential for 5-AU binding.

3.7. Role of Znβ Ion in 5-AU Binding. On the basis of the complex structure of 5-AU-PaDHPase, the Znβ ion is suggested to be critical for 5-AU binding (Figure 2). To confirm the role of Znβ in 5-AU binding and to compare the binding contribution with other mutant proteins (Table 3), we produced mono-Zn PaDHPase (Znα-PaDHPase) for binding analysis. Our crystal structure previously revealed that this mono-Zn enzyme [45] only contains a Znα ion in the active site of PaDHPase. The binding of 5-AU to Znα-PaDHPase was also analyzed by the fluorescence quenching method (Figure 4(f)). Upon the addition of 300 μM 5-AU, the intrinsic fluorescence of Znα-PaDHPase was quenched by 49.3%. The K_d value of Znα-PaDHPase for 5-AU binding was calculated to be 281.5 ± 9.0 μM from the titration curve (Figure 4(g)). Based on the K_d values, the strength of complex formation with 5-AU followed the following order: the wild-type enzyme ≈ C318A > N337A > Y155A ≈ S289A > Znα-PaDHPase (Table 3).

3.8. The 5-AU Structural Interactome. Metabolic reprogramming allows the cancer cells to rapidly proliferate, resist chemotherapies, invade, metastasize, and survive in a nutrient-deprived microenvironment [1]. Many uracil derivatives have long been used for anticancer treatment, such as 5-FU, the most commonly used pyrimidine-based antimetabolite targeting thymidylate synthase [3, 8]. 5-AU also

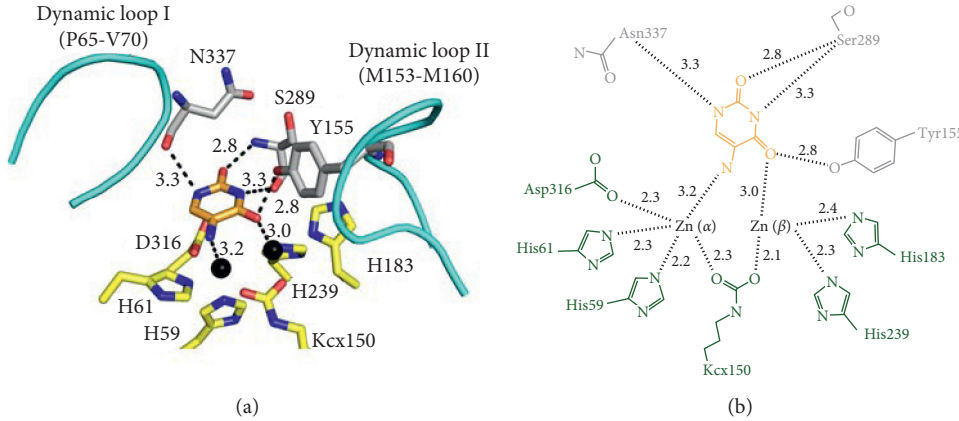

Figure 2: 5-AU binding mode. (a) The interactions of PaDHPase with 5-AU. Two metal ions (black spheres) and the substrate binding sites (gray) in PaDHPase were involved in 5-AU (light orange) binding. Dynamic loops are colored in cyan. 5-AU interacted with the main chains of residues Ser289 and Asn337 and the side chain of residue Tyr155. The distances are shown on dotted lines. (b) 5-AU interacted with Znα, Znβ, Ser289, Asn337, and Tyr155. Residues (His59, His61, Kcx150, His183, His239, and Asp316) required for metal binding are colored in green.

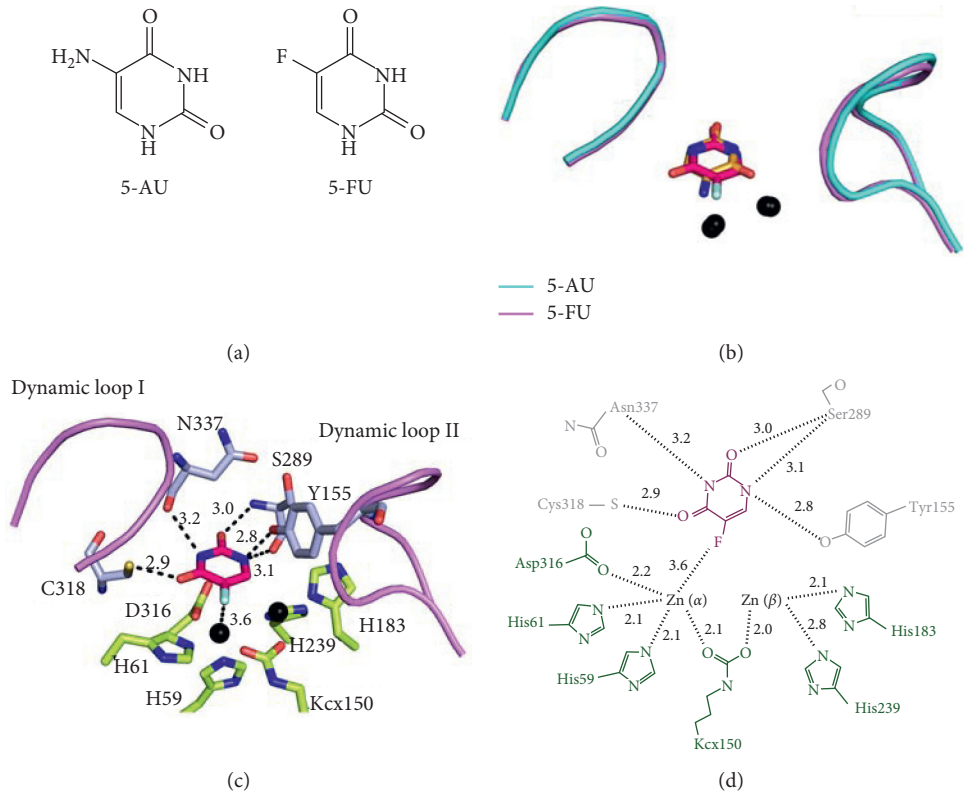

Figure 3: Comparison between the 5-AU and 5-FU binding modes. (a) The structure of 5-AU and 5-FU. (b) The superimposed structures of the 5-AU and 5-FU bound states. The conformation of the dynamic loops in both binding states is similar, but the orientations between 5-AU and 5-FU (hot pink) are different. (c) The interactions of PaDHPase with 5-FU. Znα and the substrate binding sites (gray) in PaDHPase were involved in 5-FU binding. Dynamic loops are colored in light pink. 5-FU interacted with the main chains of residues Ser289 and Asn337 and the side chains of residues Tyr155 and Cys318. The distances are shown on dotted lines. (d) 5-FU interacted with Znα, Ser289, Cys318, Asn337, and Tyr155. Residues (His59, His61, Kcx150, His183, His239, and Asp316) required for metal binding are colored in green.

possesses potent anticancer activities that can block DNA synthesis and induce replication stress [11]. 5-AU can significantly induce biphasic interphase-mitotic (IM) cells [10]. Although 5-AU and 5-FU are similar uracil derivatives, no induction of IM cells was detected even using excess 5-FU [10]. Therefore, 5-AU and 5-FU might somehow induce

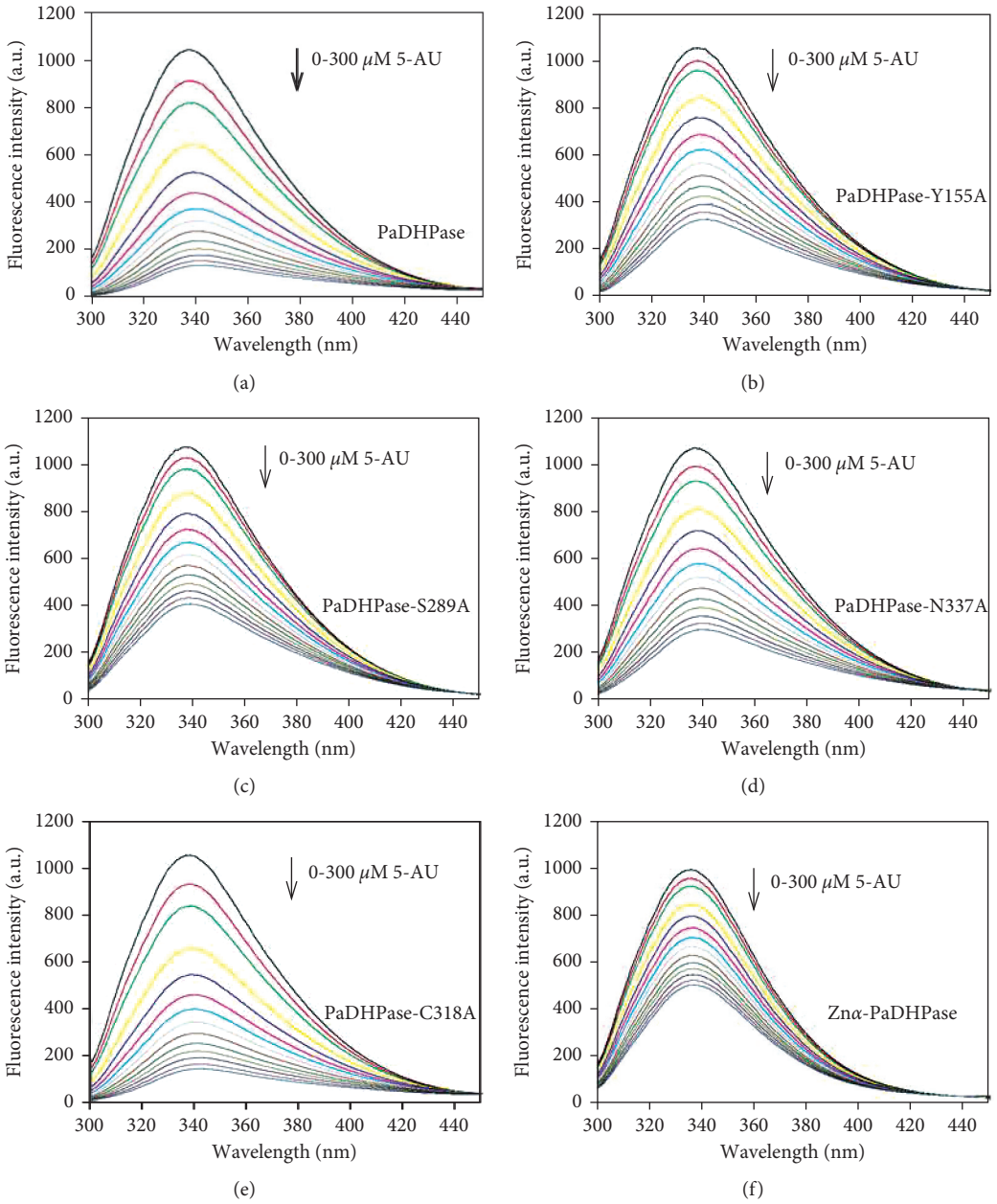

Figure 4: Continued.

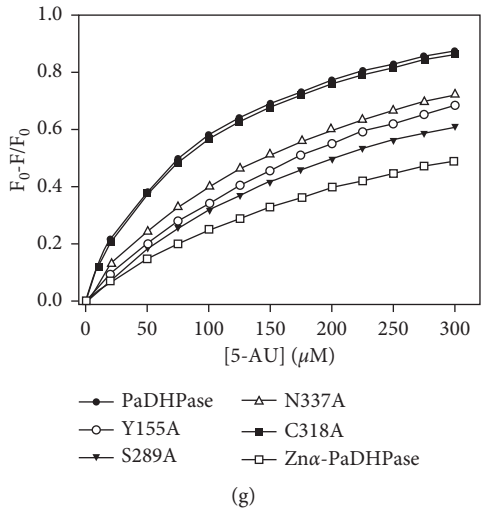

(g)

Figure 4: Fluorescence titration of PaDHPase with 5-AU. (a) The fluorescence emission spectra of PaDHPase with 5-AU of different concentrations (0–300 μM). The decrease in intrinsic fluorescence of protein was measured at 336 nm upon excitation at 279 nm with a spectrofluorimeter. The fluorescence intensity emission spectra of PaDHPase significantly quenched with 5-AU. (b) The fluorescence emission spectra of PaDHPase-Y155A with 5-AU of different concentrations (0–300 μM). (c) The fluorescence emission spectra of PaDHPase-S289A with 5-AU. (d) The fluorescence emission spectra of PaDHPase-N337A with 5-AU. (e) The fluorescence emission spectra of PaDHPase-C318A with 5-AU. (f) The fluorescence emission spectra of Znα-PaDHPase with 5-AU. (g) An aliquot amount of 5-AU was added to the enzyme solution for determining the K_d. The K_d was obtained by the equation: $\Delta F = \Delta F_{max} - K_d(\Delta F/[5\text{-AU}])$. Data points are an average of 2–3 determinations within 10% error.

Table 3: Binding parameters of PaDHPase to 5-AU.

PaDHPase	λ_{max} (nm)	λ_{em} shift (nm)	Quenching (%)	K_d value (μM)
PaDHPase	From 336.5 to 343	6.5	87.3	97.7 ± 2.0
PaDHPase-Y155A	From 336.5 to 342	6.0	68.6	247.1 ± 4.0
PaDHPase-S289A	From 337 to 339	2.0	61.6	256.0 ± 3.2
PaDHPase-N337A	From 336 to 339.5	3.5	72.4	192.1 ± 8.0
PaDHPase-C318A	From 336 to 342	6.0	86.8	103.3 ± 3.1
Znα-PaDHPase	From 335 to 336.5	1.5	49.3	281.5 ± 9.0

The decrease in the intrinsic fluorescence of ScDHOase was measured with a spectrofluorimeter (Hitachi F-2700; Hitachi High-Technologies, Japan). The K_d was obtained using the equation: $\Delta F = \Delta F_{max} - K_d(\Delta F/[5\text{-AU}])$.

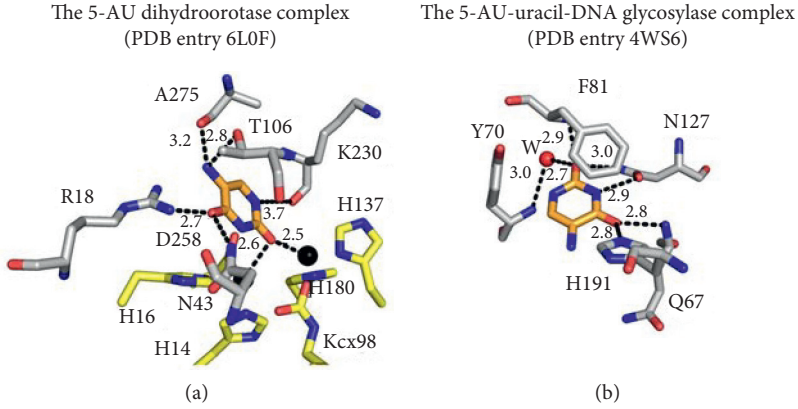

Figure 5: 5-AU binding modes. (a) The interactions of dihydroorotase with 5-AU. Two metal ions (black spheres) and the binding sites (gray) in dihydroorotase are involved in 5-AU (light orange) binding. (b) The interactions of uracil-DNA glycosylase with 5-AU.

different cellular effects. In this study, we found different binding modes of PaDHPase between 5-AU and 5-FU, and whether the different binding modes can produce distinct signaling pathways has not yet been elucidated. We noticed that other enzymes also respond to 5-AU by binding and/or inhibition. Three 5-AU-complexed protein structures are

available in the PDB for comparison: DHPase (this study), uracil-DNA glycosylase (PDB entry 4WS6), and dihydroorotase (PDB entry 6L0F). These three enzymes bind 5-AU via different binding environments (Figure 5). For example, uracil-DNA glycosylase binds 5-AU via Gln67, Tyr70, Phe81, Asn127, and His191 [50]. Dihydroorotase binds 5-AU via Arg18, Asn43, Thr106, Lys230, and Ala275 [25]. These interactions involving 5-AU binding, including that of PaDHPase-5-AU, are different. Further structural studies are needed to understand 5-AU's binding mechanisms for building the structural interactome for detailed clinical pharmacokinetics and toxicity analyses.

4. Conclusion

We identified that PaDHPase can bind 5-AU with a K_d value of 97.7 μM (Table 3 and Figure 4). The 5-AU binding mode of PaDHPase, different from that of 5-FU, was determined through structural evidence (Figure 1) and mutational analysis (Table 3). This structure provides molecular insights into how the dimetal center in PaDHPase can bind 5-AU (Figure 2). Further research can directly focus on revisiting the role of DHPase in anticancer therapy [42, 43, 51].

Data Availability

Atomic coordinates and related structure factors were deposited in the PDB with accession code 7E3U. All the data used to support the findings of this study are available from the corresponding author upon request.

Conflicts of Interest

The authors declare that they have no conflicts of interest regarding the publication of this paper.

Acknowledgments

This research was supported by grants from the Ministry of Science and Technology, Taiwan (MOST 109–2622-E-025–006 to E.S.L.) and Chung Shan Medical University (CSMU-INT-110-01 to C.Y.H.). The authors thank the experimental facility and the technical services provided by the Synchrotron Radiation Protein Crystallography Facility of the National Core Facility Program for Biotechnology, the Ministry of Science and Technology, Taiwan.

References

[1] J. Zhu and C. B. Thompson, "Metabolic regulation of cell growth and proliferation," *Nature Reviews Molecular Cell Biology*, vol. 20, no. 7, pp. 436–450, 2019.

[2] S. K. Fung and A. S. Lok, "Drug insight: nucleoside and nucleotide analog inhibitors for *hepatitis* B," *Nature Clinical Practice Gastroenterology & Hepatology*, vol. 1, no. 2, pp. 90–97, 2004.

[3] D. B. Longley, D. P. Harkin, and P. G. Johnston, "5-Fluorouracil: mechanisms of action and clinical strategies," *Nature Reviews Cancer*, vol. 3, no. 5, pp. 330–338, 2003.

[4] A. E. J. Yssel, J. Vanderleyden, and H. P. Steenackers, "Repurposing of nucleoside- and nucleobase-derivative drugs as antibiotics and biofilm inhibitors," *Journal of Antimicrobial Chemotherapy*, vol. 72, no. 8, pp. 2156–2170, 2017.

[5] S.-K. Ku, M.-C. Baek, and J.-S. Bae, "Anti-inflammatory effects of methylthiouracil in vitro and in vivo," *Toxicology and Applied Pharmacology*, vol. 288, no. 3, pp. 374–386, 2015.

[6] M.-C. Baek, B. Jung, H. Kang, H.-S. Lee, and J.-S. Bae, "Novel insight into drug repositioning: methylthiouracil as a case in point," *Pharmacological Research*, vol. 99, pp. 185–193, 2015.

[7] H.-J. Lenz, S. Stintzing, and F. Loupakis, "TAS-102, a novel antitumor agent: a review of the mechanism of action," *Cancer Treatment Reviews*, vol. 41, no. 9, pp. 777–783, 2015.

[8] P. M. Wilson, P. V. Danenberg, P. G. Johnston, H.-J. Lenz, and R. D. Ladner, "Standing the test of time: targeting thymidylate biosynthesis in cancer therapy," *Nature Reviews Clinical Oncology*, vol. 11, no. 5, pp. 282–298, 2014.

[9] P. Álvarez, J. A. Marchal, H. Boulaiz et al., "5-Fluorouracil derivatives: a patent review," *Expert Opinion on Therapeutic Patents*, vol. 22, no. 2, pp. 107–123, 2012.

[10] A. Żabka, K. Winnicki, J. T. Polit, J. Bernasińska-Słomczewska, and J. Maszewski, "5-Aminouracil and other inhibitors of DNA replication induce biphasic interphase-mitotic cells in apical root meristems of *Allium cepa*," *Plant Cell Reports*, vol. 39, pp. 1013–1028, 2020.

[11] R. M. Shaker, M. A. Elrady, and K. U. Sadek, "Synthesis, reactivity, and biological activity of 5-aminouracil and its derivatives," *Molecular Diversity*, vol. 20, no. 1, pp. 153–183, 2016.

[12] J. L. Alexander, I. D. Wilson, J. Teare, J. R. Marchesi, J. K. Nicholson, and J. M. Kinross, "Gut microbiota modulation of chemotherapy efficacy and toxicity," *Nature Reviews Gastroenterology & Hepatology*, vol. 14, no. 6, pp. 356–365, 2017.

[13] C.-Y. Huang, "Structure, catalytic mechanism, posttranslational lysine carbamylation, and inhibition of dihydropyrimidinases," *Advances in Protein Chemistry and Structural Biology*, vol. 122, pp. 63–96, 2020.

[14] J. H. Cheng, C. C. Huang, Y. H. Huang, and C. Y. Huang, "Structural basis for pH-dependent oligomerization of dihydropyrimidinase from pseudomonas aeruginosa PAO1," *Bioinorganic Chemistry and Applications*, vol. 2018, Article ID 9564391, 8 pages, 2018.

[15] C.-T. Tzeng, Y.-H. Huang, and C.-Y. Huang, "Crystal structure of dihydropyrimidinase from *Pseudomonas aeruginosa* PAO1: insights into the molecular basis of formation of a dimer," *Biochemical and Biophysical Research Communications*, vol. 478, no. 3, pp. 1449–1455, 2016.

[16] C.-Y. Huang, "Inhibition of a putative dihydropyrimidinase from *Pseudomonas aeruginosa* PAO1 by flavonoids and substrates of cyclic amidohydrolases," *PLoS One*, vol. 10, no. 5, Article ID e0127634, 2015.

[17] Y.-C. Hsieh, M.-C. Chen, C.-C. Hsu, S. I. Chan, Y.-S. Yang, and C.-J. Chen, "Crystal structures of vertebrate dihydropyrimidinase and complexes from *Tetraodon nigroviridis* with lysine carbamylation," *Journal of Biological Chemistry*, vol. 288, no. 42, pp. 30645–30658, 2013.

[18] J. Abendroth, K. Niefind, and D. Schomburg, "X-ray structure of a dihydropyrimidinase from thermus sp. at 1.3Å resolution," *Journal of Molecular Biology*, vol. 320, no. 1, pp. 143–156, 2002.

[19] B. Lohkamp, B. Andersen, J. Piškur, and D. Dobritzsch, "The crystal structures of dihydropyrimidinases reaffirm the close relationship between cyclic amidohydrolases and explain their

substrate specificity," *Journal of Biological Chemistry*, vol. 281, no. 19, pp. 13762–13776, 2006.

[20] J. A. Gerlt and P. C. Babbitt, "Divergent evolution of enzymatic function: mechanistically diverse superfamilies and functionally distinct suprafamilies," *Annual Review of Biochemistry*, vol. 70, no. 1, pp. 209–246, 2001.

[21] G.-J. Kim and H.-S. Kim, "Identification of the structural similarity in the functionally related amidohydrolases acting on the cyclic amide ring," *Biochemical Journal*, vol. 330, no. 1, pp. 295–302, 1998.

[22] A. J. Rice, R. P. Pesavento, J. Ren et al., "Identification of small molecule inhibitors against *Staphylococcus aureus* dihydroorotase via HTS," *International Journal of Molecular Sciences*, vol. 22, no. 18, p. 9984, 2021.

[23] H. H. Guan, Y. H. Huang, E. S. Lin, C. J. . Chen, and C. Y. Huang, "Complexed crystal structure of *Saccharomyces cerevisiae* dihydroorotase with inhibitor 5-fluoroorotate reveals a new binding mode," *Bioinorganic Chemistry and Applications*, vol. 2021, Article ID 2572844, 9 pages, 2021.

[24] H.-H. Guan, Y.-H. Huang, E.-S. Lin, C.-J. Chen, and C.-Y. Huang, "Plumbagin, a natural product with potent anticancer activities, binds to and inhibits dihydroorotase, a key enzyme in pyrimidine biosynthesis," *International Journal of Molecular Sciences*, vol. 22, no. 13, p. 6861, 2021.

[25] H.-H. Guan, Y.-H. Huang, E.-S. Lin, C.-J. Chen, and C.-Y. Huang, "Structural basis for the interaction modes of dihydroorotase with the anticancer drugs 5-fluorouracil and 5-aminouracil," *Biochemical and Biophysical Research Communications*, vol. 551, pp. 33–37, 2021.

[26] F. Del Caño-Ochoa and S. Ramón-Maiques, "Deciphering CAD: structure and function of a mega-enzymatic pyrimidine factory in health and disease," *Protein Science*, vol. 30, pp. 1995–2008, 2021.

[27] W.-F. Peng and C.-Y. Huang, "Allantoinase and dihydroorotase binding and inhibition by flavonols and the substrates of cyclic amidohydrolases," *Biochimie*, vol. 101, pp. 113–122, 2014.

[28] Y.-Y. Ho, Y.-H. Huang, and C.-Y. Huang, "Chemical rescue of the post-translationally carboxylated lysine mutant of allantoinase and dihydroorotase by metal ions and short-chain carboxylic acids," *Amino Acids*, vol. 44, no. 4, pp. 1181–1191, 2013.

[29] Y.-Y. Ho, H.-C. Hsieh, and C.-Y. Huang, "Biochemical characterization of allantoinase from *Escherichia coli* BL21," *The Protein Journal*, vol. 30, no. 6, pp. 384–394, 2011.

[30] K. Kim, M.-I. Kim, J. Chung, J.-H. Ahn, and S. Rhee, "Crystal structure of metal-dependent allantoinase from *Escherichia coli*," *Journal of Molecular Biology*, vol. 387, no. 5, pp. 1067–1074, 2009.

[31] C.-Y. Huang, C.-C. Hsu, M.-C. Chen, and Y.-S. Yang, "Effect of metal binding and posttranslational lysine carboxylation on the activity of recombinant hydantoinase," *JBIC Journal of Biological Inorganic Chemistry*, vol. 14, no. 1, pp. 111–121, 2009.

[32] Z. Xu, Y. Liu, Y. Yang, W. Jiang, E. Arnold, and J. Ding, "Crystal structure of d -hydantoinase from burkholderia pickettii at a resolution of 2.7 angstroms: insights into the molecular basis of enzyme thermostability," *Journal of Bacteriology*, vol. 185, no. 14, pp. 4038–4049, 2003.

[33] C.-Y. Huang and Y.-S. Yang, "A novel cold-adapted imidase from fish *Oreochromis niloticus* that catalyzes hydrolysis of maleimide," *Biochemical and Biophysical Research Communications*, vol. 312, no. 2, pp. 467–472, 2003.

[34] C.-Y. Huang and Y.-S. Yang, "The role of metal on imide hydrolysis: metal content and pH profiles of metal ion-replaced mammalian imidase," *Biochemical and Biophysical Research Communications*, vol. 297, no. 4, pp. 1027–1032, 2002.

[35] Y. S. Yang, S. Ramaswamy, and W. B. Jakoby, "Rat liver imidase," *Journal of Biological Chemistry*, vol. 268, no. 15, pp. 10870–10875, 1993.

[36] Y.-H. Huang, Y. Lien, J.-H. Chen, E.-S. Lin, and C.-Y. Huang, "Identification and characterization of dihydropyrimidinase inhibited by plumbagin isolated from *Nepenthes miranda* extract," *Biochimie*, vol. 171-172, pp. 124–135, 2020.

[37] J. S. Lee, L. Adler, H. Karathia et al., "Urea cycle dysregulation generates clinically relevant genomic and biochemical signatures," *Cell*, vol. 174, no. 6, pp. 1559–1570, 2018.

[38] S. Rabinovich, L. Adler, K. Yizhak et al., "Diversion of aspartate in ASS1-deficient tumours fosters de novo pyrimidine synthesis," *Nature*, vol. 527, no. 7578, pp. 379–383, 2015.

[39] E. R. Verrier, A. Weiss, C. Bach et al., "Combined small molecule and loss-of-function screen uncovers estrogen receptor alpha and CAD as host factors for HDV infection and antiviral targets," *Gut*, vol. 69, no. 1, pp. 158–167, 2019.

[40] M. Lee, C. W. Chan, S. C. Graham, R. I. Christopherson, J. M. Guss, and M. J. Maher, "Structures of ligand-free and inhibitor complexes of dihydroorotase from *Escherichia coli*: implications for loop movement in inhibitor design," *Journal of Molecular Biology*, vol. 370, no. 5, pp. 812–825, 2007.

[41] K. K. Seymour, S. D. Lyons, L. Phillips, K. H. Rieckmann, and R. I. Christopherson, "Cytotoxic effects of inhibitors of de novo pyrimidine biosynthesis upon *Plasmodium falciparum*," *Biochemistry*, vol. 33, no. 17, pp. 5268–5274, 1994.

[42] S. Sumi, M. Imaeda, K. Kidouchi et al., "Population and family studies of dihydropyrimidinuria: prevalence, inheritance mode, and risk of fluorouracil toxicity," *American Journal of Medical Genetics*, vol. 78, no. 4, pp. 336–340, 1998.

[43] A. B. van Kuilenburg, R. Meinsma, B. A. Zonnenberg et al., "Dihydropyrimidinase deficiency and severe 5-fluorouracil toxicity," *Clinical Cancer Research*, vol. 9, pp. 4363–4367, 2003.

[44] Y.-H. Huang, Z.-J. Ning, and C.-Y. Huang, "Crystal structure of dihydropyrimidinase in complex with anticancer drug 5-fluorouracil," *Biochemical and Biophysical Research Communications*, vol. 519, no. 1, pp. 160–165, 2019.

[45] J.-H. Cheng, Y.-H. Huang, J.-J. Lin, and C.-Y. Huang, "Crystal structures of monometallic dihydropyrimidinase and the human dihydroorotase domain K1556A mutant reveal no lysine carbamylation within the active site," *Biochemical and Biophysical Research Communications*, vol. 505, no. 2, pp. 439–444, 2018.

[46] A. J. McCoy, R. W. Grosse-Kunstleve, P. D. Adams, M. D. Winn, L. C. Storoni, and R. J. Read, "Phasercrystallographic software," *Journal of Applied Crystallography*, vol. 40, no. 4, pp. 658–674, 2007.

[47] Z. Otwinowski and W. Minor, "Processing of X-ray diffraction data collected in oscillation mode," *Methods in Enzymology*, vol. 276, pp. 307–326, 1997.

[48] J. J. Headd, N. Echols, P. V. Afonine et al., "Use of knowledge-based restraints in phenix.refine to improve macromolecular refinement at low resolution," *Acta Crystallographica Section D Biological Crystallography*, vol. 68, no. 4, pp. 381–390, 2012.

[49] P. Emsley and K. Cowtan, "Coot: model-building tools for molecular graphics," *Acta Crystallographica Section D Biological Crystallography*, vol. 60, no. 12, pp. 2126–2132, 2004.

[50] S. M. Arif, K. Geethanandan, P. Mishra, A. Surolia, U. Varshney, and M. Vijayan, "Structural plasticity in *Mycobacterium tuberculosis* uracil-DNA glycosylase (MtUng) and its functional implications," *Acta Crystallographica. Section D, Biological Crystallography*, vol. 71, pp. 1514–1527, 2015.

[51] G. D. Heggie, J. P. Sommadossi, D. S. Cross, W. J. Huster, and R. B. Diasio, "Clinical pharmacokinetics of 5-fluorouracil and its metabolites in plasma, urine, and bile," *Cancer Research*, vol. 47, pp. 2203–2206, 1987.